Chapter 4

Isolation and characterization of piscine osteonectin and downregulation of its expression by parathyroid hormone-related protein

Co-authors:

Begoña Redruello, Josep Rotllant, Pedro M. Guerreiro, Liliana I. Anjos, Adelino V.M. Canário and Deborah M. Power

Published in *Journal of Bone and Mineral Research* (2005), **20**, 682-692

4.1 Introduction

In teleost fishes, calcified structures such as bone and scales account for 99% of the total body calcium which is present primarily as complexes of calcium carbonate and calcium phosphate (Wendelaar Bonga and Pang, 1991). Two types of mineralized structures can be distinguished depending on their origin, dermal or endochondral. Structures of dermal origin result from the condensation of sclerotomal cells on the surface of the primary notochord sheath and the subsequent deposition of calcium. Examples of this differentiation model are vertebrae centra and neurocranial bones. Endochondral bone initially develops as a cartilage template which then ossifies. Structures that follow this model are vertebrae arches and caudal rays (Kardong, 1998). Scales of most teleost fishes are subepithelial calcified structures of mesodermal origin, and structurally consist of an upper osseous layer impregnated with calcium salts and a lower fibrous plate (Fouda, 1979). Fish scales contain both formative cells (scleroblasts or osteoblasts) and resorptive cells (scleroclasts or osteoclasts) and are analogous to the mammalian building-resorption model (Bereiter-Hahn and Zylberberg, 1993, Sire, *et al.*, 1990).

The skeleton in fish not only provides mechanical support but may also serve as a calcium reservoir in periods of extra demand such as during vitellogenesis and/or when uptake of environmental calcium becomes energetically unfavourable (Björnsson, *et al.*, 1999). Mobilization of calcium from scales and the vertebral skeleton has been shown in salmonids during the spawning migration from calcium-rich seawater to freshwater (Kacem, *et al.*, 2000, Persson, *et al.*, 1998) and as a result of treatment of rainbow trout, *Oncorhynchus mykiss*, with estrogen (Lehane, *et al.*, 1995). Moreover, osteoclast-specific tartrate-resistant acid phosphatase (TRACP) activity is increased in 17β-estradiol (E_2)-treated goldfish, *Carassius auratus*, scales *in vitro* (Suzuki, *et al.*, 2000) and *in vivo* (Suzuki and Hattori, 2002) whereas melatonin (Suzuki and Hattori, 2002) and calcitonin (Suzuki, *et al.*, 2000) suppress this enzymatic activity, suggesting a protective mechanism against excess degradation of the scale calcified matrix during vitellogenesis (Suzuki, *et* *al.*, 2000). The role of other hormones involved in calcium mobilization from fish scales are poorly characterized, as is the role of extracellular matrix (ECM) proteins in this process.

In mammals the ECM is fairly well characterized and is composed of a highly complex arrangement of structural proteins, proteoglycans, latent or active growth factors, and matricellular proteins. The latter comprise a non-homologous, function-based family of regulatory factors that include osteonectin (OSN), osteopontin, thrombospondins 1 and 2, tenascins C and X, and the recently described OSN-related proteins, SC1 and QR1. OSN is a multifunctional metal-binding glycoprotein encoded by a single-copy gene that displays a high degree of interspecies sequence conservation. OSN expression has been used as a marker of the osteoblastic response since its first description as a linker between mineral and collagen in human bone (Termine*, et al.*, 1981b). OSN is implicated in mineralization of bone and cartilage (Pacifici*, et al.*, 1990) and high concentrations of calcium ions increase expression of OSN and other markers of terminal differentiation, followed by an increased production of mineral matrix. An OSN-deficient mouse strain has recently been described, which has progressive severe osteopenia as a result of decreased osteoblast and osteoclast numbers and a decreased bone formation rate (Delany*, et al.*, 2000, Delany*, et al.*, 2003). Furthermore, the main hypercalcaemic factor in higher vertebrates, parathyroid hormone (PTH), exerts a negative control on OSN gene expression in rat osteosarcoma cell lines (Noda and Rodan, 1987). Although piscine homologs of PTH cDNA have recently been reported in puffer fish (Danks*, et al.*, 2003) and zebrafish (Gensure*, et al.*, 2004), their biological functions remain to be defined. This means that parathyroid hormone-related protein (PTHrP) is, to date, the only identified hypercalcaemic factor in teleost fish (Flanagan*, et al.*, 2000, Guerreiro*, et al.*, 2001, Power*, et al.*, 2000) although its actual role in fish skeletal homeostasis remains to be established. The role of OSN as a key factor in bone remodelling in tetrapods makes it an excellent marker to evaluate the action of PTHrP on the teleost skeleton.

The objectives of the present study were: 1) to isolate OSN mRNA from sea bream (*Sparus auratus*), 2) to study its expression in mineralized tissues, and 3) to determine the effect of PTHrP treatment on OSN gene expression in sea bream scales.

4.2 Material and Methods

4.2.1 Fish maintenance and tissue sampling

Sea bream were maintained at Estação Marinha do Ramalhete (Universidade do Algarve, Portugal) under natural conditions of water temperature (17-25ºC), photoperiod and salinity (36-40 ‰), as described in section 2.1. Animal care was in accordance with the ethical guidelines of the Animal Behaviour Society (The Association for the Study of Animal Behaviour (ASAB) and Animal Behaviour Society (ABS), 2003) and National legislation. Tissue sampling was carried out as presented in section 2.2. For mRNA extraction tissues were frozen in liquid nitrogen and stored at -80℃ until use. Tissues for histology and *in situ* hybridization (ISH) were fixed in fresh 4% paraformaldehyde overnight at 4ºC (section 2.2). Before processing, calcified tissues (vertebra, operculum, skull and gills) were decalcified in 0.5M EDTA pH 8.0 (appendix I), for 8 to 40 days and washed with DEPC water (appendix I). Tissues were then embedded in paraffin and 7µm sections were cut and mounted on APES (3-aminopropyltriethoxysilane) treated slides (for details see appendix II).

4.2.2 Construction of an intervertebral tissue cDNA library from *S. auratus*

Total RNA was extracted from intervertebral tissue collected from sea bream individuals of a range of different sizes (individual weight range, 150-3500g) using TRI reagent (Sigma-Aldrich). The mRNA fraction was isolated from total RNA by chromatography on oligo(dT) cellulose columns (Amersham Biosciences). A directional cDNA library was made using 3µg mRNA isolated from intervertebral tissue and ZAP-cDNA Gigapack III Gold Cloning kit (Stratagene). Average insert size was 1450 bp as determined by PCR analysis of 40 randomly selected recombinants. The titre of the primary library was 9×10^5 plaque-forming units (pfu) per 500µl.

4.2.3 Cloning and characterization of OSN cDNA from *S. auratus*

An oligonucleotide primer pair (sbOSNfw1: 5'-GGTCATCGTGGAAGAGCC-3' and sbOSNrv2: 5'-TGTGTGGGTCAGGTATCC-3') designed on the basis of a multiple alignment (ClustalX, Thompson, *et al.*, 1997) of all the available full length nucleotide sequences for OSN mRNA (see below) was used in a RT-PCR to amplify a 685 bp cDNA fragment from *S. auratus* intervertebral tissue. This cDNA was found to comprise the complete coding sequence of OSN except for the last 159 nucleotides and was subsequently used as a probe to screen the intervertebral tissue cDNA library. Five pBlueScript SK(+)-based clones (among 2×10^3 pfus) were isolated and automatically sequenced. Database searches using the BLAST algorithm (Altschul, *et al.*, 1997) confirmed their identity as OSN cDNAs, but only one was full-length. The full-length sequence was submitted to the EMBL database (accession number AJ564190) and is designated sbOSN throughout this chapter.

4.2.4 *In silico* analysis

A search for the complete coding sequence of OSN in public databases yielded eleven sequences: human (*Homo sapiens*, NM003118), bovine (*Bos Taurus*, NM174464), rat (*Rattus norvegicus*, NM012656), mouse (*Mus musculus*, BC057324), quail (*Coturnix coturnix*, AF077327), chicken (*Gallus gallus*, L24906), African clawed frog (*Xenopus laevis*, X62483), rainbow trout (*Oncorhynchus mykiss*, V25721), fruit fly (*Drosophila melanogaster*, NM143252), a crustacean (*Artemia franciscana*, AB052961) and a nematode (*Caenorhabditis elegans*, NM067638). To widen the phylogenetic analysis the protein sequence of OSN was subject to TBLASTN (Altschul, *et al.*, 1997) against the genomic databases of puffer fish (*Fugu rubripes*; http://fugu.hgmp.mrc.ac.uk) and the primitive chordate *Ciona intestinalis* (http://genome.jgi-psf.org/ciona). Putative OSN was found in *Fugu* scaffold M002731 and *Ciona* scaffold ci0100136414. The HGMP Nix interface (Williams G., Woollard, P. and Hingamp, P., unpublished data; http://www.hgmp.mrc.ac.uk/NIX/) was used to analyze gene organization and to deduce amino acid sequences. A multiple sequence alignment of the available

OSN amino acid sequences, including that of sea bream, was used as the input data for phylogenetic analysis using the Neighbour Joining Method (Saitou and Nei, 1987) via the PAUP interface (v. 4.0, Swofford, 1998). The phylogenetic output was displayed using Treetool (Cole*, et al.*, 2003).

4.2.5 Semi-quantitative RT-PCR and Northern Blot

Total RNA was extracted from individual samples of adult sea bream tissues (intervertebral disc, vertebrae, skull bone, branchial arch, scale, caudal rays, operculum, brain, heart, liver, head-kidney, kidney, duodenum, mid-gut, hind-gut, gonad, white muscle and gill filaments) using TRI reagent. For skeletal structures, mechanical disruption in liquid nitrogen was carried out before to RNA extraction.

First strand cDNA synthesis was performed using 3µg of total RNA and the M-MuLV reverse transcriptase procedure (Gibco BRL). RT-PCR reactions were carried out as described in section 2.6. The specific sbOSN primers used were sbOSNfw1 (5'-GGTCATCGTGGAAGAGCC-3') and sbOSNrv1 (5'-GCAGGAG GTGTCGTAGGT-3'). A cycle number optimization was carried out in order to run a non-saturated amplification protocol, consisting of an initial denaturing step of 95ºC for 2 minutes followed by 22 cycles at 95ºC for 30 seconds, 55ºC for 30 seconds, 72ºC for 45 seconds and a final elongation step at 72ºC for 5 minutes. To estimate relative quantity of sbOSN gene expression the ratio sbOSN/ribosomal RNA (18S) was determined. 18S primers (18Sfw: 5'-TCAAGAACGAAAGTCGGAGG-3', 18Srv: 5'-GGACATCTAAGGGCATCACA-3') were used in separate PCR reactions with a similar amplification protocol to sbOSN but with fewer (18) cycles. Amplified products were separated on agarose gels and their signals quantified by densitometry (section 2.6).

For Northern blot analysis, 10µg of total RNA per tissue was hybridized using the radiolabelled 685 bp sbOSN cDNA probe following the protocol described in section 2.7.

4.2.6 *In situ* hybridization (ISH)

To characterize tissue morphology, transverse serial sections of vertebrae centrum and bones of the neurocranium, adjacent to those used for *in situ* hybridization, were stained using general histological procedures. Vertebra sections were stained with haematoxylin and eosin (section 2.3.1) and the skull bone sections were stained simultaneously with alcian blue 8 GX, haematoxylin and van Gieson solution (section 2.3.4) which stain cartilage blue, nucleus purple and collagen of osseous tissue red, respectively.

For preparation of a riboprobe for *in situ* hybridization, a pBlueScript SK(+) vector containing the full length sbOSN cDNA (1073 bp) was linearized by digestion with *Bgl*II endonuclease (Promega). The 3' probe obtained was approximately 400 bp in length. The linearized vector was purified and *in vitro* transcription was carried out as described in section 2.4.1. The riboprobe was resuspended in 25µl of RNase and DNase free sterile water (Sigma-Aldrich).

In situ hybridization was carried out following the protocol presented in section 2.4.2. Transverse sections of operculum, gill arch, vertebrae centrum and bones of the neurocranium as well as whole scales were pre-hybridized at 58ºC for 2 h in hybridization solution (appendix I). Tissues were then hybridized overnight at 58ºC in hybridization solution containing approximately $3\mu g ml^{-1}$ of riboprobe. Stringency washes to remove non hybridized probe were carried out at the hybridization temperature, twice with 2×SSC (appendix I) for five minutes and then with 1×SSC for five minutes. Hybridized probe was detected using NBT and BCIP as chromagens. Control experiments were performed by treating samples with RNase prior to hybridization with the riboprobe and/or by omitting riboprobe from the reaction.

4.2.7 *In vitro* sea bream scales bioassay

Scales from the dorsolateral region were collected from sea bream individuals (n=4) after anaesthesia with 2-phenoxyethanol (0.01% in seawater, Sigma-Aldrich) by plucking them from the epidermis with forceps and collecting into buffered physiological saline. Pools of approximately 20 scales (30-50mg) were incubated in 24-well sterile culture plates (Costar, Corning) in 1ml.well^{-1} of MEM (Sigma-Aldrich), pH 7.4. All the experiments were performed at room temperature (23ºC) in an oxygen-saturated atmosphere.

Measurements of cAMP production to demonstrate scale viability

Sea bream scales were incubated for 30 minutes with MEM-IMBX (1mM) containing 1µM Forskolin or 10nM piscine (1-34)-PTHrP alone or in combination with 10nM piscine (7-34)-PTHrP (Genemed Synthesis). Harvested scales were then re-suspended in 0.01M PBS with 4mM EDTA, sonicated and aliquots taken for protein determination. Subsequently samples were boiled, centrifuged at 5000rpm for 5 minutes and the supernatant was removed and stored at -20ºC until analysis. The cAMP concentration in samples was determined using the Biotrak TRK 432 kit (Amersham Biosciences). Results are reported as picomoles of cAMP per miligram of total protein.

Effect of PTHrP on OSN expression in scales

Pools of sea bream scales (n=4) were incubated for 8 hours in MEM medium alone (control samples) or MEM containing piscine (1-34)-PTHrP at 10nM or 1000nM (treated samples). The scales were harvested and frozen at -80ºC until total RNA extraction for RT-PCR analysis of sbOSN expression.

4.2.8 Statistics

Results are presented as mean ± SEM. Data analysis of incubation studies was carried out using one-way analysis of variance (ANOVA) followed by the Student-Newman-Keuls (SNK) test; significance was considered at $p<0.05$.

4.3 Results

4.3.1 Characterization and phylogenetic analysis of sea bream OSN cDNA

The full-length sbOSN clone isolated from the intervertebral cDNA library encompasses 1073 bp, including an open reading frame (ORF) of 912 bp starting at nucleotide +58 and ending with a stop codon TAA at nucleotide +970. A conserved translational start site (Kozak, 1986) surrounds the ATG initiation codon including A at position -3. However, a polyadenylation consensus sequence was not found in the 3'UTR region (Figure 4.1). Indeed, sea bream OSN cDNA is shorter than its mammalian counterparts and this difference is probably because of its shorter 3'UTR, because the coding region has an equivalent size (Table 4.1). The ORF encodes 304 amino acids including a stretch of 17 amino acids at the N-terminus of the predicted protein that conforms well to the signal peptide consensus sequence and ends with a signal peptidase cleavage site (Nielsen*, et al.*, 1997).

Table 4.1 - Characteristics of known osteonectin cDNAs and corresponding proteins. Sizes of all known osteonectin cDNAs, including 5' and 3' untranslated regions (UTR) and coding regions are indicated. Sea bream osteonectin is in bold. The horizontal broken line separates vertebrates from invertebrates.

Species	Tissue	cDNA size	5'UTR (bp)	cds (bp)	3'UTR (bp)	Protein size (aa)		Accession number
						Signal peptide	Mature	
S. auratus	**Intervertebral cartilage**	**1073**	**57**	**912**	**104**	**17**	**287**	**AJ564190**
H. sapiens	Bone	2133	57	912	1164	17	287	NM003118
B. taurus	Embryo	2141	54	915	1172	17	288	J03233
R. norvegicus	Kidney	981	68	906	nd	17	285	D28875
M. musculus	Embryo	1153	78	909	166	17	286	BC004638
G. gallus	Embryo	1009	43	897	69	17	281	L24906
C. coturnix	Embryo	2123	48	897	1178	17	282	AF077327
X. laevis	Embryo	1557	nd	903	654	17	284	X62483
O. mykiss	Brain	1431	85	903	443	17	284	U25721
D. melanogaster	Embryo	1170	109	915	146	20	285	NM143252
A. franciscana	Embryo	1083	51	876	156	20	272	AB052961
C. elegans	Embryo	1109	18	795	296	20	245	NM067638

Note: bp, base pairs; a.a., amino acid residues; nd, not defined

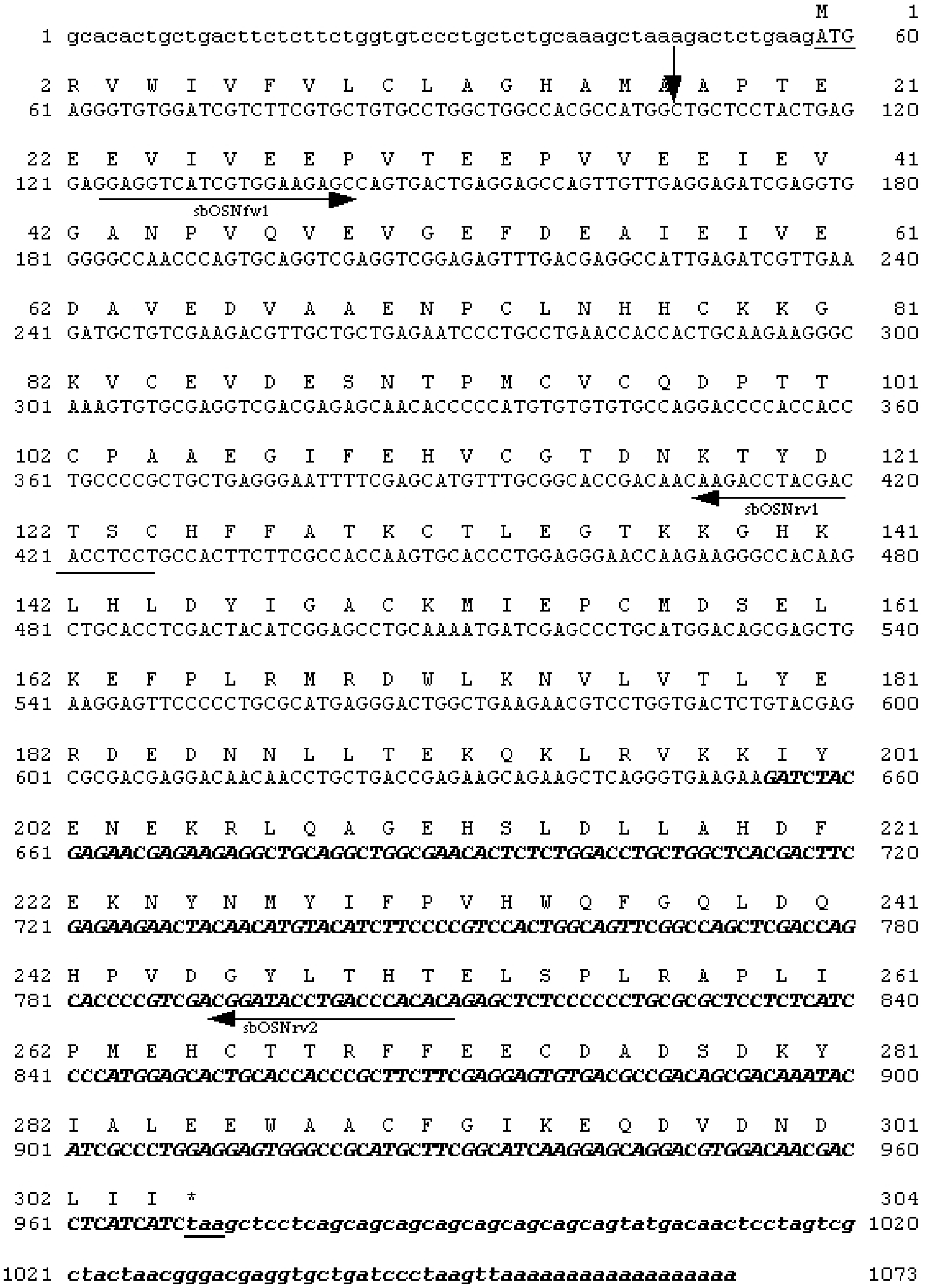

```
                                                            M       1
   1 gcacactgctgacttctcttctggtgtccctgctctgcaaagctaaagactctgaagATG   60

   2 R  V  W  I  V  F  V  L  C  L  A  G  H  A  M  A  A  P  T  E    21
  61 AGGGTGTGGATCGTCTTCGTGCTGTGCCTGGCTGGCCACGCCATGGCTGCTCCTACTGAG  120

  22 E  E  V  I  V  E  E  P  V  T  E  E  P  V  V  E  E  I  E  V    41
 121 GAGGAGGTCATCGTGGAAGAGCCAGTGACTGAGGAGCCAGTTGTTGAGGAGATCGAGGTG  180
                 sbOSNfw1
  42 G  A  N  P  V  Q  V  E  V  G  E  F  D  E  A  I  E  I  V  E    61
 181 GGGGCCAACCCAGTGCAGGTCGAGGTCGGAGAGTTTGACGAGGCCATTGAGATCGTTGAA  240

  62 D  A  V  E  D  V  A  A  E  N  P  C  L  N  H  H  C  K  K  G    81
 241 GATGCTGTCGAAGACGTTGCTGCTGAGAATCCCTGCCTGAACCACCACTGCAAGAAGGGC  300

  82 K  V  C  E  V  D  E  S  N  T  P  M  C  V  C  Q  D  P  T  T   101
 301 AAAGTGTGCGAGGTCGACGAGAGCAACACCCCCATGTGTGTGTGCCAGGACCCCACCACC  360

 102 C  P  A  A  E  G  I  F  E  H  V  C  G  T  D  N  K  T  Y  D   121
 361 TGCCCCGCTGCTGAGGGAATTTTCGAGCATGTTTGCGGCACCGACAACAAGACCTACGAC  420
                                                          sbOSNrv1
 122 T  S  C  H  F  F  A  T  K  C  T  L  E  G  T  K  K  G  H  K   141
 421 ACCTCCTGCCACTTCTTCGCCACCAAGTGCACCCTGGAGGGAACCAAGAAGGGCCACAAG  480

 142 L  H  L  D  Y  I  G  A  C  K  M  I  E  P  C  M  D  S  E  L   161
 481 CTGCACCTCGACTACATCGGAGCCTGCAAAATGATCGAGCCCTGCATGGACAGCGAGCTG  540

 162 K  E  F  P  L  R  M  R  D  W  L  K  N  V  L  V  T  L  Y  E   181
 541 AAGGAGTTCCCCCTGCGCATGAGGGACTGGCTGAAGAACGTCCTGGTGACTCTGTACGAG  600

 182 R  D  E  D  N  N  L  L  T  E  K  Q  K  L  R  V  K  K  I  Y   201
 601 CGCGACGAGGACAACAACCTGCTGACCGAGAAGCAGAAGCTCAGGGTGAAGAAGATCTAC  660

 202 E  N  E  K  R  L  Q  A  G  E  H  S  L  D  L  L  A  H  D  F   221
 661 GAGAACGAGAAGAGGCTGCAGGCTGGCGAACACTCTCTGGACCTGCTGGCTCACGACTTC  720

 222 E  K  N  Y  N  M  Y  I  F  P  V  H  W  Q  F  G  Q  L  D  Q   241
 721 GAGAAGAACTACAACATGTACATCTTCCCCGTCCACTGGCAGTTCGGCCAGCTCGACCAG  780

 242 H  P  V  D  G  Y  L  T  H  T  E  L  S  P  L  R  A  P  L  I   261
 781 CACCCCGTCGACGGATACCTGACCCACACAGAGCTCTCCCCCCTGCGCGCTCCTCTCATC  840
                   sbOSNrv2
 262 P  M  E  H  C  T  T  R  F  F  E  E  C  D  A  D  S  D  K  Y   281
 841 CCCATGGAGCACTGCACCACCCGCTTCTTCGAGGAGTGTGACGCCGACAGCGACAAATAC  900

 282 I  A  L  E  E  W  A  A  C  F  G  I  K  E  Q  D  V  D  N  D   301
 901 ATCGCCCTGGAGGAGTGGGCCGCATGCTTCGGCATCAAGGAGCAGGACGTGGACAACGAC  960

 302 L  I  I  *                                                   304
 961 CTCATCATCtaagctcctcagcagcagcagcagcagcagcagtatgacaactcctagtcg 1020

1021 ctactaacgggacgaggtgctgatccctaagttaaaaaaaaaaaaaaaaaa          1073
```

Figure 4.1 - Nucleotide and deduced amino acid sequence of sbOSN cDNA. Nucleotides (lower row) and amino acids (single-letter notation, upper row) are numbered on both the left- and the right-hand side of the sequence rows. The untranslated regions are in lowercase and the open reading frame in uppercase. The start (ATG) and stop (TAA) codons are underlined. In the peptide sequence, the pro/mature cleavage site is marked by a vertical arrow. Horizontal arrows signal the localization of sbOSNfw1, sbOSNrv1 and sbOSNrv2 primers. The cDNA fragment used as a probe for *in situ* hybridization is shown in italic bold.

A multiple sequence alignment performed with the available vertebrate OSN amino acid sequences (accession numbers in Table 4.1) is shown in figure 4.2. OSN is very similar among all vertebrates, with an overall percentage identity between sea bream and human of 77%, not very different from the 81% identity between sea bream and rainbow trout, another teleost (Table 4.2). Comparison of sbOSN to OSN from organisms without a skeleton such as the primitive chordate *C. intestinalis* and the invertebrate *C. elegans* revealed low homology which was 38% and 33% identity, respectively. The amino acid sequence of module I is too poorly conserved to produce pairwise alignments (Table 4.2).

Table 4.2 - Comparison of amino acid sequence similarity for osteonectin proteins. Values represent overall and structural modules % amino acid identity of pairwise sequence alignments. The (-) in module I column indicates that homology was too low to obtain pairwise alignment.

Species	Overall	Module I	Module II	Module III
H. sapiens	77	53	83	84
O. mykiss	81	46	86	92
F. rubripes	85	76	85	93
C. intestinalis	38	30	41	47
D. melanogaster	29	-	30	33
A. franciscana	29	-	25	31
C. elegans	33	-	32	34

Structurally, sea bream OSN contains a signal peptide (residues 1-17) and the three characteristic modules and motifs described for this protein (Figure 4.2): module I (residues 20-69) corresponding to the highly acidic N-terminal region (Lane and Sage, 1994), module II (residues 70-150), a follistatin-like domain that includes an epidermal growth factor-like and a Kazal protease inhibitor-like motifs as well as a N-glycosylation site at Asn117 (Hohenester, *et al.*, 1997); and module III (residues 151-304) which is the C-terminus extracellular Ca^{2+}-binding module and contains a pair of EF-hand motifs (Busch, *et al.*, 2000). sbOSN also contains 14 conserved cysteines, 10 in module II and 4 in module

III (Figure 4.2). A *Fugu* genome database search yielded a scaffolds M002731 in which the gene organization was fully characterized, comprised of nine exons and eight introns.

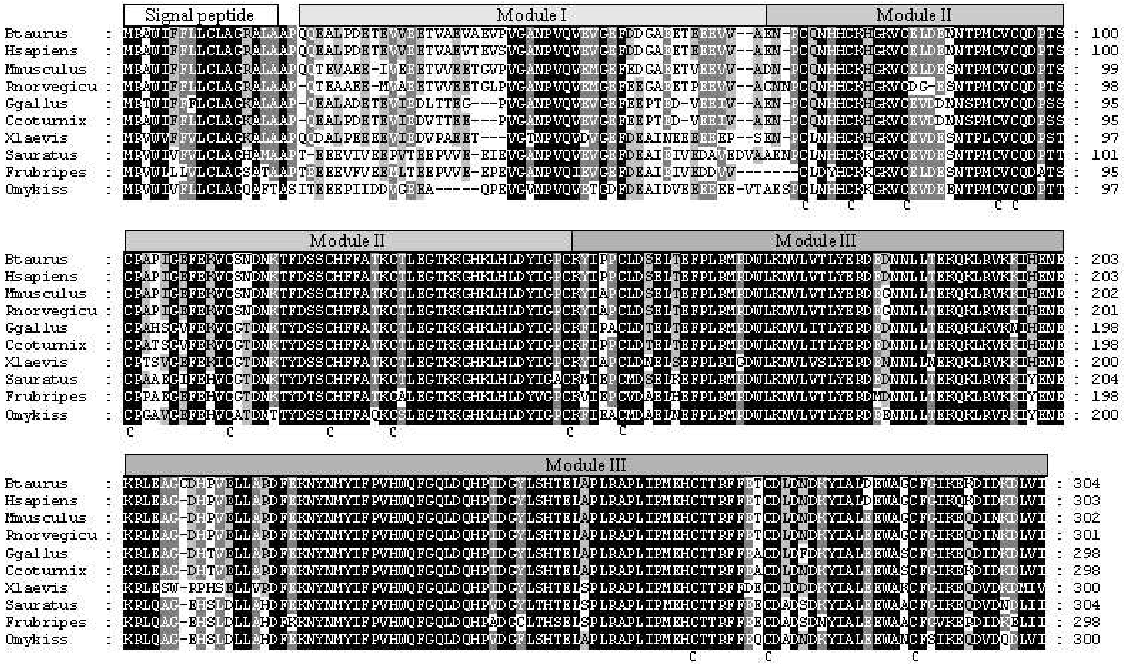

Figure 4.2 - Multiple sequence alignment of OSNs from tetrapods and fishes. The signal peptide is composed of the first 17 amino acid residues in all the proteins. An upper row grey colour intensity scale indicate the three characteristic modules: **I** (residues 3 to 52 of the mature protein), **II** (residues 53-133) and **III** (residues 134-287). Fourteen conserved cysteine residues are indicated with a 'C' below.

The deduced amino acid sequence of sbOSN is 85% identical to *Fugu* OSN. These results are in conformity with the expected evolutionary distance between organisms and were confirmed by a phylogenetic analysis performed using the Neighbour Joining method (Figure 4.3) with rat hevin, (accession number AAA68708), an OSN family-related protein, as the outgroup. Two major clades were found that correspond to the division between invertebrate and vertebrate OSN sequences. sbOSN is grouped with the other piscine OSNs within the vertebrate clade, while *C. intestinalis* OSN is grouped within the invertebrate clade.

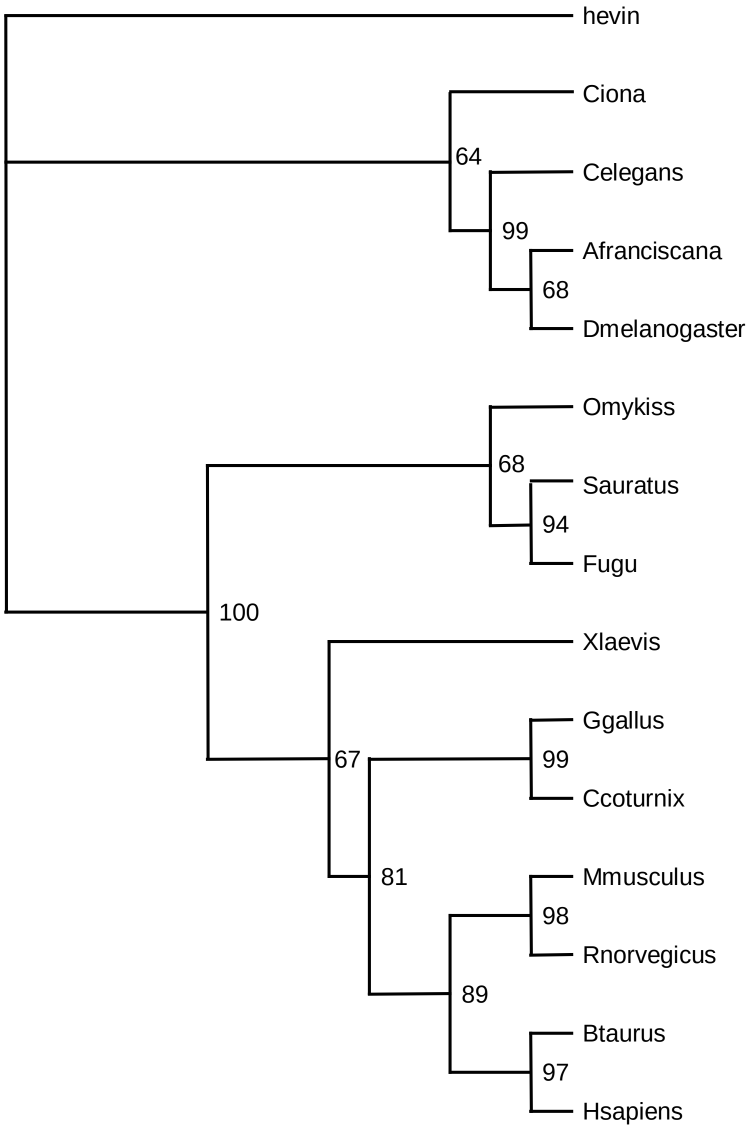

Figure 4.3 - Phylogenetic rooted tree of known OSNs obtained using the Neighbour Joining method and with rat hevin protein as outgroup.

4.3.2 sbOSN mRNA tissue expression

Semi-quantitative RT-PCR indicated that sbOSN is most abundant in calcified tissues (Figure 4.4 A) and the scales, intervertebral disc and the vertebrae have the highest level of expression, followed by the caudal rays, branchial arches and opercular bone. Of all the calcified tissue analysed the neurocranium has the lowest level of OSN expression which is similar in abundance to that observed in the soft tissues, brain and gonad. The remaining soft tissues analysed have almost undetectable OSN mRNA, and the liver has the lowest expression. Northern blot analysis revealed a single transcript of sbOSN of approximately 1.3 Kb in all the tissues analysed (Figure 4.4 B). The relative abundance of OSN in tissues is similar to that observed in the semi-quantitative RT-PCR analysis.

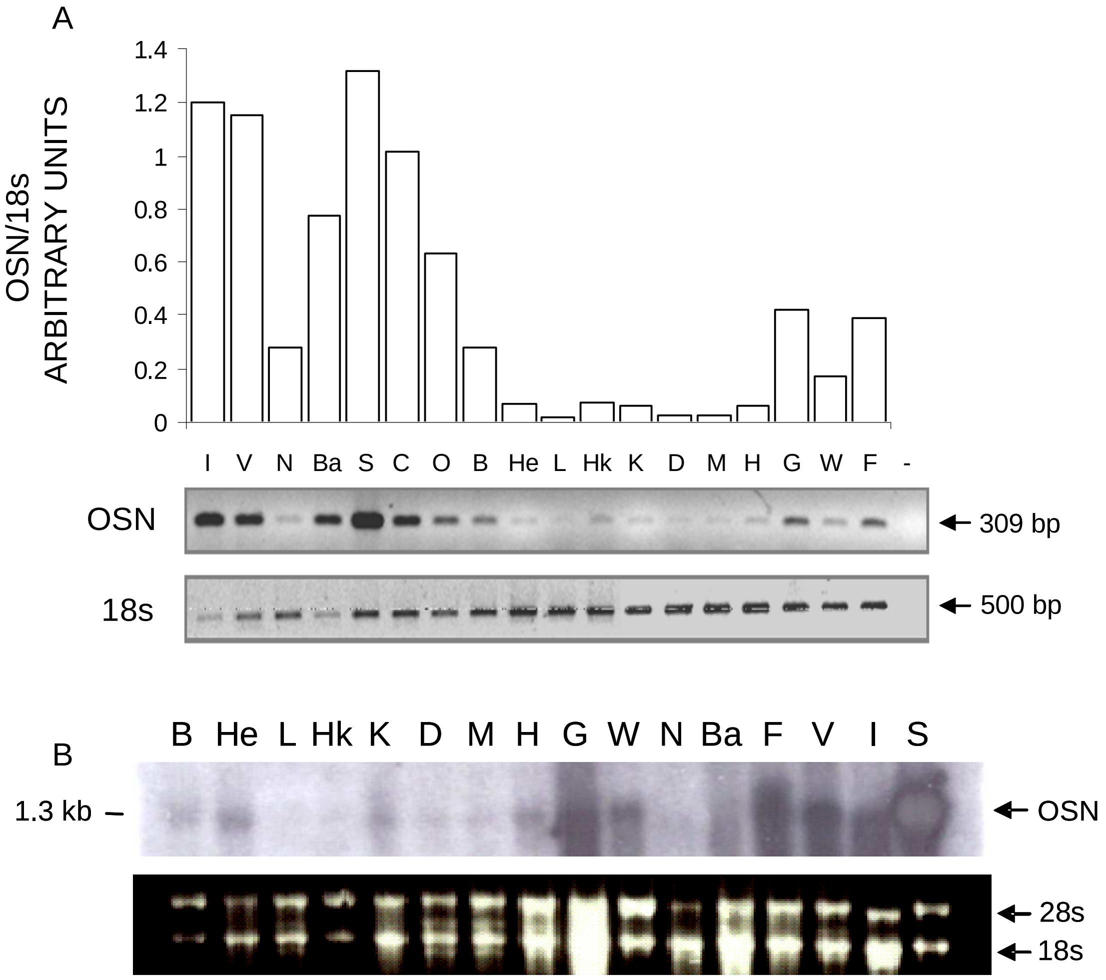

Figure 4.4 - sbOSN expression in adult tissues. A) Relative abundance of sbOSN determined by semi-quantitative RT-PCR, with 18S to normalize quantity of total RNA in the different tissues. B) Northern blot analysis (upper panel) of sbOSN tissue distribution showing the presence of a specific transcript of 1.3 kb. The lower panel shows the ethidium bromide staining of the agarose gel used for blotting which demonstrates that the loading of all lanes was similar and the integrity of the RNAs. Tissues: I-intervertebral disc; V-vertebrae centrum; N-frontal bone of the neurocranium; Ba-branchial arch; S-scale; C-caudal ray; O-opercular bone; B-brain; He-heart; L-liver; Hk-headkidney; K-kidney; D-duodenum; M-mid gut; H-hind gut; G-gonad; W-white muscle; F-gill filaments; (-) - control without reverse transcriptase.

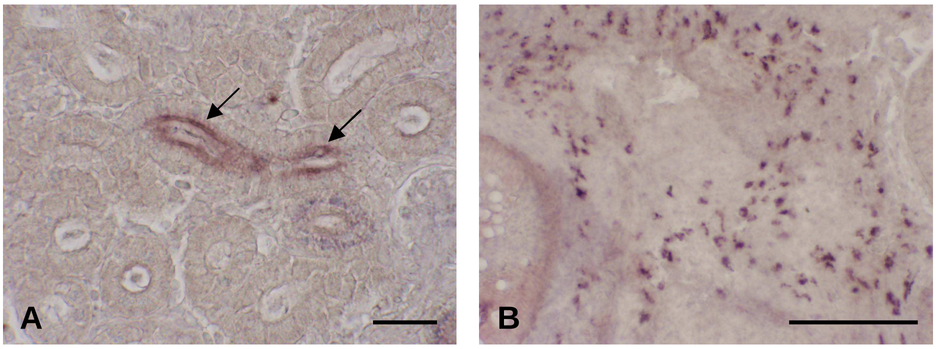

Figure 4.5 - *In situ* hybridization of sbOSN in adult kidney (A) and mid gut (B). In the kidney signal is observed in cells of some kidney tubules (A, arrows). Unidentified cells in the *lamina propria* of the mid gut expressed OSN mRNA (B). Scale bars: 50µm.

In situ hybridization confirmed that OSN mRNA is scarce in soft tissues such as heart, liver, kidney, head kidney, gastrointestinal tract and gonads, although a weak signal is detected occasionally in all these tissue. OSN mRNA was detected in cells of kidney tubules (Figure 4.5 A) and in unidentified cells of the *lamina propria* of the mid gut (Figure 4.5 B). OSN mRNA is principally present in tissues with a structural role such as operculum (Figure 4.6 A and B), scales (Figure 4.6 C and D), gill filaments (Figure 4.6 E), gill arches (Figure 4.6 G), vertebrae (Figure 4.7 B) and skull bone (Figure 4.7 D). No signal is detected in any of the controls for probe specificity (Figure 4.6 F and H). In the operculum, OSN mRNA expression is detected in the cytoplasm of cells localized in the basement membrane layer of the epidermis, adjacent to the dermis and also in some cells at the extreme edge of the epidermis (Figure 4.6 A and B). No signal is observed in the underlying dermis or in differentiated cells of the epidermis. In scales (Figure 4.6 C and D), OSN mRNA is abundantly expressed in the scleroblasts present at the interface between the fibrous and the bony layer but appeared to be absent from the overlying epidermis. In the gills (Figure 4.6 E), OSN mRNA is localized in unidentified cells distributed along the secondary lamellae and did not appear in the chloride cells that are located at the base of lamellae. In the gills (Figure 4.6 G), an intense OSN signal is also present in what appeared to be the cytoplasm of the endothelial cells lining the numerous blood vessels in this region. However, further observations revealed that the signal was in fact present in unidentified structures located in the gill rakers. In the vertebrae, OSN mRNA is observed to be abundant in cells of the basement membrane of the epithelium that coats the neural canal (Figure 4.7 B). However, it is absent from bone or calcifying tissue in this region. In the skull, bones localized in the anterior-frontal region of the neurocranium showed affinity for alcian blue 8 GX as well as for van Gieson solution confirming it is composed of both cartilaginous and osseous tissues (Figure 4.7 C). OSN mRNA is abundant in the presumptive chondrocytes at the transition layer between cartilage and bone and also in some scattered presumptive chondrocytes of this tissue (Figure 4.7 D).

4.3.3 Effect of PTHrP on sbOSN expression in fish scales

Fish scales have a relatively simple tissue structure being composed primarily of epidermis that does not appear to express OSN (see *in situ* results) and scleroblasts that do. The scales can be readily removed without damage to the fish and subsequently regrow. The viability of the scales *in vitro* was shown by incubation with forskolin (1µM), a selective activator of adenylyl-cyclase, which greatly increased the intracellular level of cAMP (Figure 4.8 A).

The presence of PTHrP signalling in the scales was also showed in incubations *in vitro* by measuring of cAMP production in response to (1-34)-PTHrP stimulation. Piscine (1-34)-PTHrP (10nM) evoked an approximately 5-fold rise in cAMP in sea bream scales (Figure 4.8 A). This stimulatory effect of (1-34)-PTHrP on cAMP release could be blocked by an excess (1000nM) of the antagonist (7-34)-PTHrP. (1-34)-PTHrP treatment at both 10nM and 1000nM greatly reduced OSN mRNA expression in scales, whereas the untreated controls retained constant high levels of OSN expression after 8 hours of incubation (Figure 4.8 B).

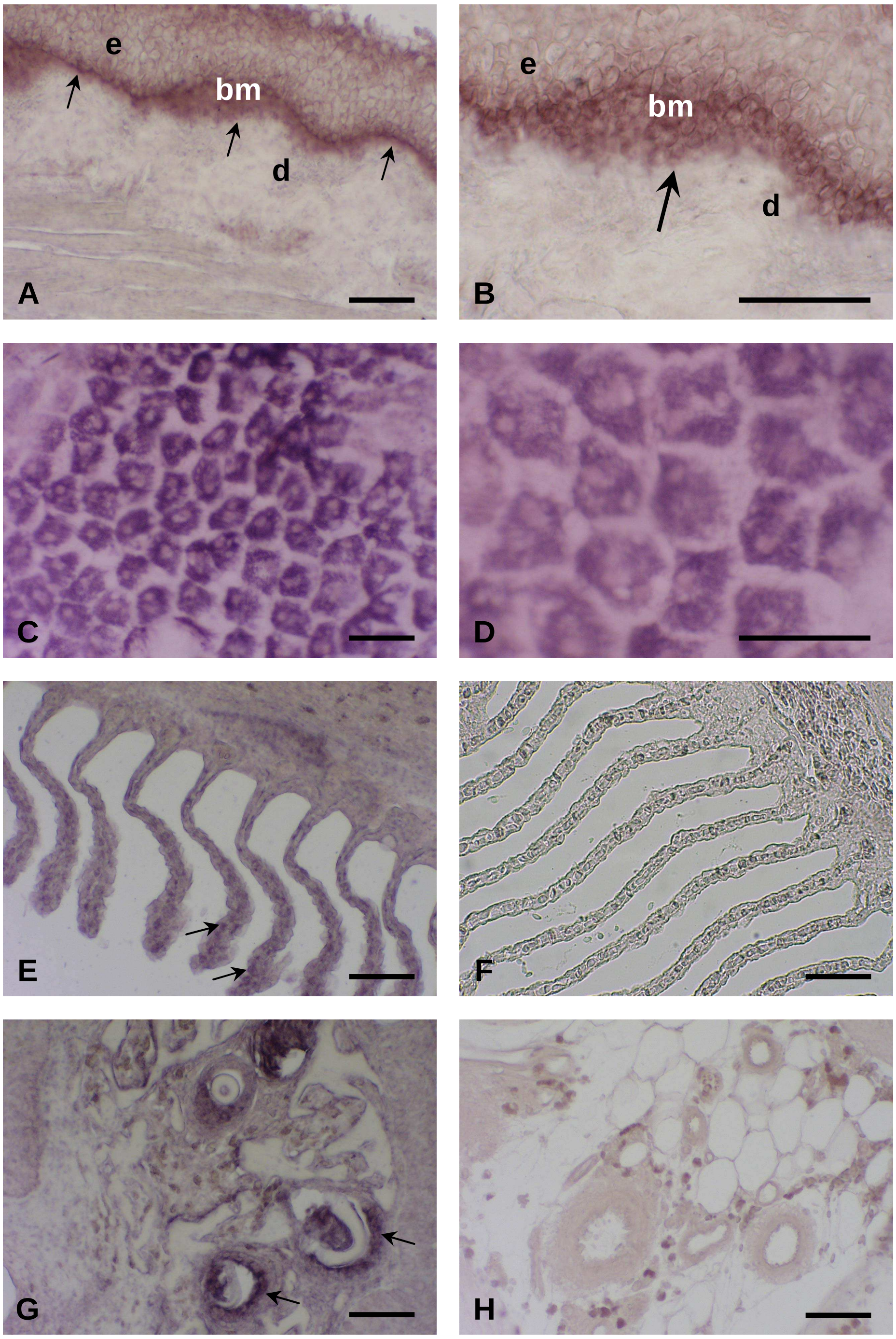

Figure 4.6 - *In situ* hybridization of sbOSN in adult operculum (A, B), scales (C, D), gill lamellae (E) and gill arches (G). In the operculum the most intense signal is observed in the basement membrane of the epidermis (A and B, arrows). An intense signal is observed in the scleroblasts of the scale (C and D). Unidentified cells in the gill secondary lamellae expressed OSN mRNA (E). In the gills the signal is also detectable in unidentified structures located in the gill rakers (G). No signal is detected in the negative control of gill filaments and gill arches (F and H). B and D are magnifications of A and C, respectively. e: epidermis; bm: basement membrane; d: dermis. Scale bars: 50µm.

4.4 Discussion

Comparison of the main features of sbOSN with that of other vertebrates and invertebrates revealed that the most remarkable characteristic is the 3'UTR region, which is ten times shorter than its mammalian or avian homologs. Because a polyadenylation signal was not found in the cDNA sequence, the possibility of sbOSN being a truncated clone remains open. The existence of alternative transcripts could also explain the differences in length to vertebrate OSNs although this is unlikely because, in the Northern blot, only a 1.3 kb transcript was detected in all tissues analysed (see Figure 4.4 B). Furthermore, to our knowledge, no alternative OSN mRNA transcripts have been described in vertebrates. From the analysis of available public databases genomes, a gene encoding an OSN ortholog composed of 9 exons spanning the coding sequence was identified in *Fugu rubripes*, and the same organization was found in human and mouse, suggesting a common ancestor for all the vertebrates. In the tunicate *C. intestinalis*, 7 exons span the OSN coding sequence for the same number and type of OSN domains as in vertebrates, indicating a rearrangement of the exon-intron boundaries between tunicates and vertebrates. In *C. elegans* 6 exons span the OSN coding region.

Multiple sequence alignment indicated that the deduced amino acid sequence of sbOSN shares identical structure with its vertebrate counterparts, and it is composed of three characteristic modules. Module I is highly acidic with 14-15 glutamic acid residues in mammals and binds 5-8 Ca^{2+} with low affinity (Brekken and Sage, 2000, Lane and Sage, 1994). It interacts with hydroxyapatite and is implicated in the mineralization of cartilage and bone (Brekken and Sage, 2000, Lane and Sage, 1994). In sea bream this region contains 17 glutamic acid residues and most likely has functions comparable to those in the higher vertebrates. In contrast, this module is highly divergent among invertebrates and this may be associated with a reduced affinity of OSN for calcium ions, as noted in *C. elegans* (Schwarzbauer and Spencer, 1993). The absence of a mineralized skeleton in the primitive chordate *C. intestinalis* might also explain the phylogenetic association of its OSN with that of invertebrates (Figure 4.3) supporting the hypothesis that OSN has evolved to acquire novel roles in relation to the development of an internal skeleton. The follistatin-like domain of module II includes in its core a Kazal protease inhibitor-like region and an EGF-like motif through which it can interact with proteoglycans and may be important for binding to cell surface receptors (Hohenester*, et al.*, 1997). The functions ascribed to this region include inhibition of proliferation of endothelial cells (Funk and Sage, 1993) and stimulation of endothelial proliferation and angiogenesis (Iruela-Arispe*, et al.*, 1996).

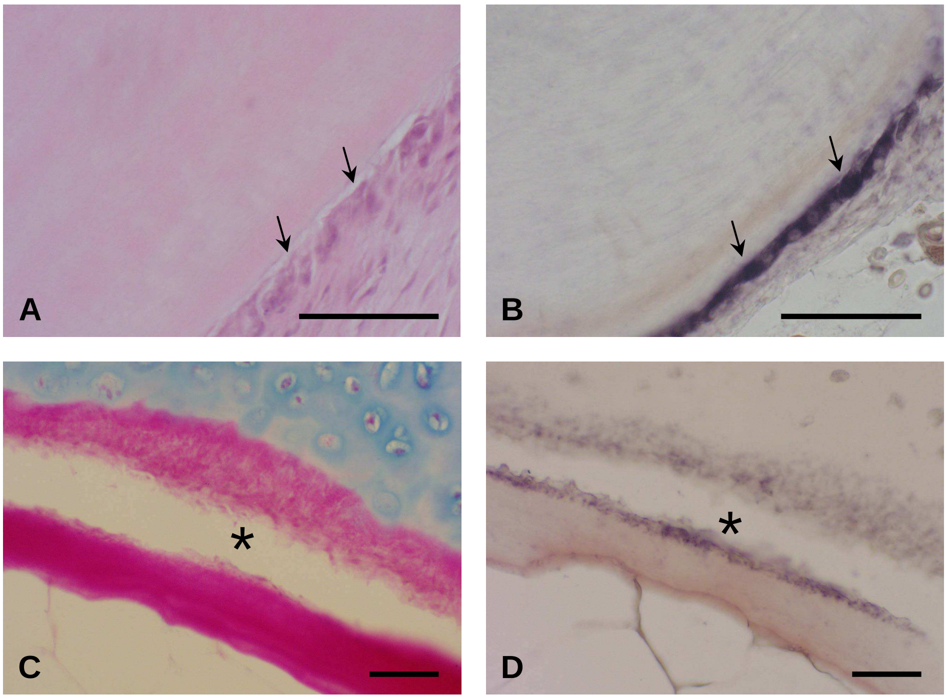

Figure 4.7 - *In situ* hybridization of sbOSN in adult vertebrae and neurocranium. A) Haematoxylin and eosin staining of transverse section of vertebrae to highlight morphology. B) In the vertebrae sbOSN mRNA is restricted to the basement membrane of the epithelia which lines the neural canal (arrows). C) Skull section simultaneously stained with alcian blue 8 GX, haematoxylin and van Gieson solution showing cartilage in blue, the nucleus purple and the collagen in osseous tissue red. D) In the skull sbOSN mRNA is localized in the presumptive chondrocytes of the transition layer (*) between cartilage and bone. Slight damage to this tissue during processing has split the transition layer. Scale bars: 50µm.

In all vertebrates, including the sea bream, the C-terminal module III contains two EF-hand motifs with high affinity for extracellular Ca^{2+} (Maurer*, et al.*, 1992) and through which OSN binds collagen types I, III and IV in a Ca^{2+}-dependent fashion (Brekken and Sage, 2000). This module has been implicated in the inhibition of cell proliferation through the interaction and sequestering of crucial factors such as platelet-derived and vascular endothelial growth factors. The tertiary structure of OSN is maintained by 7 disulphide bridges provided by 14 conserved cysteines and stabilized by calcium binding to the two EF-hand motifs (Busch*, et al.*, 2000). The high conservation of sequence and structure strongly suggests that the role of OSN as a cell-cell and cell-matrix communication regulator has been well conserved in fish and tetrapods.

OSN mRNA has a ubiquitous presence in sea bream adult tissues. The high levels of sbOSN found primarily in mineralizing tissue is consistent with what has been described in higher vertebrates where OSN has been implicated in mineralization and osteoblastic-lineage differentiation (Delany*, et al.*, 2000, Delany*, et al.*, 2003). Osteonectin was shown to support bone remodelling and the maintenance of bone mass in mice. OSN-null mice have a decrease in osteoclast and osteoblast surface with a decreased bone formation leading to development of osteopenia (Delany*, et al.*, 2000). The marrow stroma from OSN-null mice contains fewer osteoblastic precursor cells and, in these animals, osteoblasts do not achieve a fully mature phenotype, which is evidenced by decreased abundance of osteocalcin mRNA and decreased responsiveness to parathyroid hormone (PTH; Delany*, et al.*, 2003). It is the high affinity of OSN for calcium and collagen that has been proposed to be important in the control of matrix mineralization and in the synthesis and assembly of the basement membrane (Delany*, et al.*, 2000, Delany*, et al.*, 2003, Holland*, et al.*, 1987). Both the function and structure of osteonectin are modulated by Ca^{2+} ions. Binding of Ca^{2+} causes a change in conformation that alters its affinity for collagen (Yan and Sage, 1999).

Osteonectin has already been shown to be present in several teleost fish tissues (Tang and McKeown, 1997) but its expression was not studied in mineralized fish tissues. Among the sea bream calcified tissues, the highest levels of sbOSN expression were detected in scales, in the cytoplasm of hexagonal and single nucleated cells (see Figure 4.6 D), supporting the idea of osteoblast-like cells being the source of OSN in sea bream scales. It is likely that these same cells express other osteoblast markers which have been detected in scales such as collagen type 1 (Redruello, unpublished) and bone γ-carboxyglutamic acid protein (Suzuki, *et al.*, 2000).

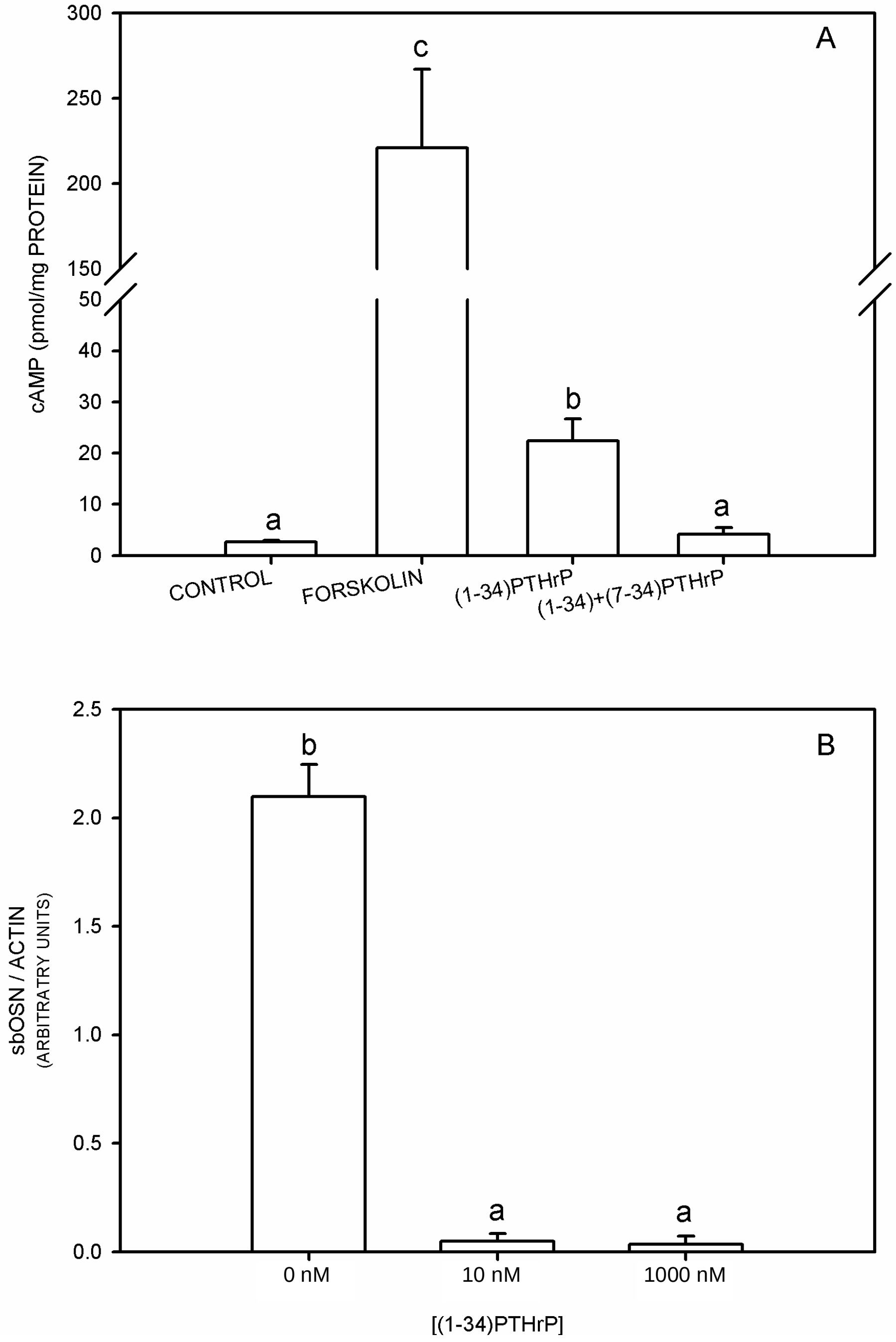

Figure 4.8 - Effect of PTHrP on sea bream scales *in vitro*. A) cAMP production in response to treatment with (1-34)-PTHrP (10nM) and (7-34)-PTHrP (1000nM). B) sbOSN mRNA expression in response to treatment with (1-34)-PTHrP. Bars are means ± SEM of 4 separate experiments and different letters represent significant differences.

The fish operculum and gills are specialized structures for gas exchange and uptake and elimination of ions and water. In order to carry out these functions the gills are exposed to a continuous flow of water and are subjected to a high epithelium turnover rate. The localization of abundant sbOSN mRNA in the basement membrane and epithelial cells in this tissue may be associated with its important role in cell movement and proliferation (Brekken and Sage, 2000). OSN mRNA seemed to be found in the endothelial cells of the blood vessels present in the gill arches and such observations could indicate that OSN in fish, in common with observations in mammals, was involved in angiogenesis and regulation of endothelial barrier function (Brekken and Sage, 2000, Goldblum*, et al.*, 1994, Iruela-Arispe*, et al.*, 1995). A similar role has also been proposed for rainbow trout OSN (Tang and McKeown, 1997). However, careful observations of the results in posterior studies revealed that the OSN mRNA expression detected was associated with unidentified structures present in the gill rakers pointing to a different role of OSN in the gills. Further studies need to be carried out to elucidate this question. Both rainbow trout (Tang and McKeown, 1997) and sea bream OSN transcripts are detected also in brain and gonads. The appearance of osteonectin in early stages of development suggests an involvement of this extracellular protein in brain development probably related to cellular proliferation and migration (Tang and McKeown, 1997). Although an explanation for the presence of OSN in the gonads has yet to be found, in normal adult human tissue its expression is associated with the basement membranes of tissue undergoing remodelling and replacement, such as the gut, mammary gland and steroidogenic adrenal, follicular and Leydig cells (Brekken and Sage, 2000, Holland*, et al.*, 1987).

To study the regulatory pathways that might control OSN expression in calcified structures, we have used sea bream scales in an *in vitro* bioassay. Scales have the advantage of 1) possessing high levels of OSN mRNA, 2) being readily removed and cultured, 3) having a relatively simple tissue organization and 4) containing mineralized tissue that acts as a calcium storage pool of physiological importance in fish (Weiss and Watabe, 1979). Fish scales are composed of an upper osseous layer impregnated with calcium phosphate and a lower fibrous plate (Fouda, 1979) where scleroclasts and scleroblasts bring about, respectively, the mobilization and deposition of calcium.

The mineral content of the scales may therefore be mobilized for physiological use, although the role of hormones in this process is still largely unknown (Kacem*, et al.*, 2000, Lehane*, et al.*, 1995, Persson*, et al.*, 1998). One of the hormones potentially acting on calcium metabolism in the scales is PTHrP, which has been cloned in sea bream (Flanagan*, et al.*, 2000) and a peptide corresponding to the 1-38 amino acids of the N-terminal region of piscine PTHrP was found to increase whole body calcium influx and decrease efflux in larvae (Guerreiro*, et al.*, 2001). Furthermore, sea bream PTHrP levels in the circulation are high compared to humans, and the pituitary is a potential main source of this hormone (Rotllant*, et al.*, 2003). Such observations may indicate that PTHrP is the teleost fish equivalent to tetrapod PTH in the hypercalcaemic regulation of calcium. In tetrapods, the N-terminal region of PTH also exerts a negative control on the mineralization process as well as on the levels of expression of some anabolic proteins such as OSN (Swarthout*, et al.*, 2002). As shown in this study, sea bream scales respond to PTHrP with a sizeable increase in cAMP accumulation. This is a specific effect that can be abolished by the PTHrP receptor antagonist (7-34)-PTHrP. Furthermore, PTHrP, both at physiological (10nM) and pharmacological (1000nM) concentrations, abolished OSN mRNA synthesis. This is strong evidence that the OSN promoter is a target for a PTHrP-mediated signalling pathway. In contrast, human PTHrP failed to have any effects on OSN expression in a goldfish scale cell line (Lehane*, et al.*, 1999). This is not surprising since only 18 of the 34 amino acids of the N-terminal sequence of the human molecule are similar to piscine PTHrP (Flanagan*, et al.*, 2000). Furthermore, we have shown that changes in a single amino acid at the extremity of the N-terminal domain of piscine PTHrP can result in loss or lack of functionality (Rotllant*, et al.*, 2005). Altogether, these results suggest that, in teleost fish, PTHrP may control the mineralization process in scales through the regulation of some key genes, such as OSN. This is analogous to the function of PTH in bone mineralization in higher vertebrates and suggests that scale and bone metabolism share essential features.

The high calcium turnover in teleost fish scales indicates they can act as stores for calcium to be released during periods of special requirements such as during starvation or reproduction (Suzuki and Hattori, 2002). We suggest that both PTHrP, and possibly other factors (Suzuki*, et al.*, 2000, Suzuki and Hattori, 2002), through OSN participate in this process.

In conditions of high extracellular calcium, calcium sensing receptor signalling (Flanagan*, et al.*, 2002) would result in downregulation of PTHrP, allowing OSN upregulation and calcium deposition in the scale ECM. The reverse, release of calcium from the fish scales, would occur when calcium is present at low levels. However, the elucidation of molecular and cellular mechanisms underlying calcium deposition and mobilization, and OSN function in fish scale ECM require further investigation.

Acknowledgments of practical work

M. D. Estêvão carried out histology and *in situ* hybridization and acknowledges the contribution of B. Redruello and L. I. Anjos for the construction of the cDNA library, for cloning and characterizing sbOSN and for the Northern blot analysis, and J. Rotllant and P. M. Guerreiro for the *in vitro* scales bioassay.